

Prestressed Morphing Bistable and Neutrally Stable Shells

Keith A. Seffen¹

Senior Lecturer
e-mail: kas14@cam.ac.uk

Simon D. Guest

Reader
e-mail: sdg13@cam.ac.uk

Department of Engineering,
University of Cambridge,
Trumpington Street,
Cambridge CB2 1PZ, UK

This study deals with prestressed shells, which are capable of “morphing” under large deflexions between very different load-free configurations. Prestressing involves plastically curving a flat, thin shell in orthogonal directions either in the opposite or same sense, resulting in two unique types of behavior for isotropic shells. Opposite-sense prestressing produces a bistable, cylindrically curved shell provided the prestress levels are large enough and similar in size: This effect forms the basis of a child’s “flick” bracelet and is well known. On the other hand, same-sense prestressing results in a novel, neutrally stable shell provided the levels are also sufficiently large but identical: The shell has to be made precisely, otherwise, it is monostable and is demonstrated here by means of a thin, helically curved strip. The equilibrium states associated with both effects are quantified theoretically and new expressions are determined for the requisite prestress levels. Furthermore, each stability response is revealed in closed form where it is shown that the neutrally stable case occurs only for isotropic materials, otherwise, bistability follows for orthotropic materials, specifically, those, which have a shear modulus different from the isotropic value. Finally, prestressing and initial shape are considered together and, promisingly, it is predicted that some shells can be neutrally stable and bistable simultaneously. [DOI: 10.1115/1.4002117]

1 Introduction

Figures 1 and 2 show two simply-made thin metallic shells with unusual structural properties. First, there is a *bistable* disk with two distinct out-of-plane cylindrical shapes. It is formed by plastically coiling a flat disk around a cylindrical former in orthogonal directions but in *opposite* senses. The coiling process does not have to be exact and the disk can be a different material: Bending the disk manually achieves the same end-point and stiff paper card, such as a beer mat, can be used instead. Afterward, although initially reluctant to deform, the shell then snaps through between shapes. Second, there is a *neutrally stable* strip, which can, when carefully positioned, rest in one of several helical configurations as shown, each being cylindrically coiled about the lengthwise axis of strip, with a radius approximately equal to the transverse curvature of the straightened strip. The manufacturing process was described by Guest et al. [1], which is similar to the bistable case except that the original flat strip is curved plastically along and across itself in the *same sense* in a very precise manner. The neutral behavior can be felt by twisting the strip along its length by hand where an absence of torsional rigidity becomes evident: A long, rectangular section amplifies the helical curving but the effect is preserved in shells with other planforms but identically made. Thus, the two responses differ because of the residual stresses left behind after cold-working and what is remarkable is that they can be very different by simply reversing the direction of plastic coiling. These shells demonstrate simple morphing structures, which can be used to create effective shape-changing—large deflexion—technologies with unique load-free equilibrium configurations.

The aim of this study is to understand the factors governing the performance of these shells. In relation to the first case, Kebabze et al. [2] considered a thin strip, stress-free and initially curved across its width, which is, then, plastically coiled back on itself to create bistability. Most of their study is spent extracting the profile of residual stresses left behind after prestressing: Then, assuming

an *inextensible* deformation mode, they confirm the opposite-sense and orthogonal curvature of the second equilibrium shape for the particular prestress distribution. On the other hand, Mansfield [3,4] recorded a performance akin to neutral stability for a heated lenticular shell, initially free of stresses and flat but subjected to uniform thermal gradients through its thickness. He shows that the shell either bends equally in all directions for low gradients or it becomes highly curved under severe heating about a single axis whose direction is *indeterminate*.

This study is not concerned with the mechanics of the prestressing process itself, rather, it assumes for simplicity that prestressing imparts *uniform* residual bending stresses to the shell before any elastic deformation, which must follow for self-equilibration without applied loads. The analytical formulation, therefore, accounts for prestress in a simple way but it generally accounts for in-plane stretching even though inextensible deformations are often justified for very thin shells. Such asymptotic behavior can be observed as the limiting case of certain solutions, as will be shown. As well as describing the equilibrium shapes of shell, the stability conditions for each case in Figs. 1 and 2 can be obtained in closed form and the responsible physical mechanism can be identified, which would not be straightforward to do using, for example, a finite element analysis. Accordingly, these conditions can be compared to those for the inextensible shell in Ref. [2] or can formally confirm the neutral stability in Refs. [3,4].

Each case is detailed in Secs. 3 and 4, respectively, after sketching the formulation in Sec. 2, which has been derived elsewhere by the first author. Even though practical shells are isotropic, the material shear modulus is generally specified during solution of the governing equations and the reason is connected to a finding by Seffen [5] who showed that *annealed* shells of the same material constitution are bistable if they have the right amount of initial out-of-plane curvature. Specifically, if there is sufficient positive Gaussian curvature as in cap-like shells, simple isotropic shells are bistable but saddle-shaped, stress-free shells with negative Gaussian curvature are bistable only by increasing the shear modulus and the corresponding rise in the torsional stiffness of the shell helps to restrain or lock the deformed shape.

Prestressing of initially flat shells produces equilibrium states whose stability performance is very different to the effects of initial shape even though prestress and initial shape are similarly

¹Corresponding author.

Contributed by the Applied Mechanics of ASME for publication in the JOURNAL OF APPLIED MECHANICS. Manuscript received August 20, 2009; final manuscript received July 2, 2010; accepted manuscript posted July 7, 2010; published online October 8, 2010. Assoc. Editor: Matthew R. Begley.

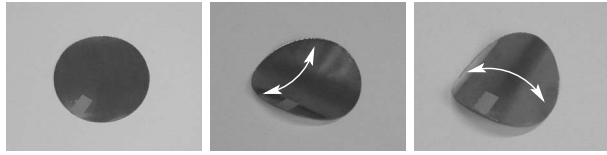


Fig. 1 A thin, prestressed bistable smooth shell of diameter 50 mm and thickness 0.1 mm and made from thin age-hardened copper beryllium sheet. Left: the original flat metallic disk—note the rectangular sticker tab fashioned to the upper surface. Middle: the curved shell after plastic coiling around a pencil stem. Right: a second curved shape of shell, formed by plastic coiling in the opposite direction, about an axis at right angles to the middle shape. The shell is subsequently bistable between the final two curved shapes.

expressed in the governing equations of deformation. Such behavior has not been reported and it usefully extends the previously known results: The difference is due to the presence or absence of initial Gaussian curvature and not to the final equilibrium shapes. Specifically, it is shown that bistability under opposite-sense prestressing, which attempts to cause negative Gaussian curvature, is not affected by the value of the shear modulus whilst same-sense prestressing, which deforms the shell to a positive Gaussian curvature, results in neutral stability for an isotropic value only.

Furthermore, these solutions assume that the shell has been identically prestressed in orthogonal directions, as suggested after making several physical samples where, as noted originally, neutrally stable shells are difficult to make when prestress levels are not equal due to manufacturing imperfections. The sensitivity of performance due to *disparate* prestressing is therefore considered but a valuable conclusion emerges when the shear modulus is permitted to vary, which augments an earlier conclusion—that neutrally stable behavior arises only when prestress levels are identical and when the shell is isotropic. This is carried out in Sec. 5.

For completeness, a last exercise is considered in Sec. 6 for spherically curved shells and then prestressed in the same sense. This shows that the originally flat neutrally stable shell is part of a family of similarly performing shells but where additional stable shapes exist, depending on the size of the initial spherical curvature.

Before closing the introduction, there are two final points to make. First, the analysis requires simplifying but justifiable assumptions for the sake of transparency, which are explained in Ref. [6] and summarized as follows. The material is linearly elastic and the strains remain small although the displacements can be large, relative to the thickness of the shell. The initial and deformed curvatures are uniform over the bulk of the shell in the absence of externally applied loads and any practical boundary

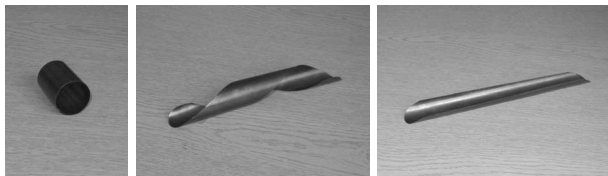


Fig. 2 Three views of a neutrally stable shell-strip made by plastically coiling the original flat strip along and across its length [1]. In each view, the strip rests such that it is coiled about an axis inclined to the strip length at: left, 90 deg to become fully coiled; middle, approximately 45 deg to form a spiral; right, 0 deg to yield an open strip. The transition between shapes is effected by twisting the strip between its ends and there is no stiffness. The strip is made from age-hardened copper beryllium sheet and has a length of 180 mm; the radius of coiling is approximately 11 mm.

layer of nonuniform deformation near the edge of shell is neglected due to its relatively small thickness, which is taken to be constant throughout. For further mathematical expediency, the shell has an elliptical planform with major and minor semi-axes parallel to orthogonal coordinates x and y , respectively. The governing equations, which are algebraic in nature, are carefully treated to reveal, as far as possible, solutions in closed form. The second point concerns an earlier study by Guest and Pellegrino [7] on finding bistable shells in a range of materials, which are not prestressed or heated but which are uniform in shape—similar to the materials used here. Their analysis is compact yet general but it differs from the present study in several ways. They assume inextensibility from the outset, which leads to the assumption that all equilibria must be cylindrically curved. Accordingly, bistable shapes need to be described by only two parameters—the direction and orientation of the cylindrical curvature, and this allows the strain energy stored in the shell to be determined straightforwardly. Rather than solve explicitly for equilibria, they show that new shapes can be found by graphical inspection of the strain energy landscape and their stability is inferred from the performance of the local contours. The present study explicitly solves nonlinear and coupled governing equations of deformation for new equilibrium shapes. For large displacements, inextensibility follows in the limiting sense and the shells tend to cylindrical forms but, otherwise, the shape is generally captured by two independent curvatures and a twisting curvature. Of course, some of the findings in Ref. [7] can be duplicated if the prestress is set to zero but the reader is referred to the findings in Ref. [5] for a more direct comparison of results with Guest and Pellegrino [7].

2 Governing Equations of Deformation

From Seffen [6], the governing equations of deformation for an elliptical shell undergoing relatively large displacements are

$$\bar{\kappa}_x + \mu \bar{\kappa}_y = \bar{\kappa}_{x0} + \nu \bar{\kappa}_{y0} + \bar{\kappa}_{xF} + \nu \bar{\kappa}_{yF} \quad (1a)$$

$$\mu \bar{\kappa}_x + \bar{\kappa}_y = \nu \bar{\kappa}_{x0} + \bar{\kappa}_{y0} + \nu \bar{\kappa}_{xF} + \bar{\kappa}_{yF} \quad (1b)$$

$$(2\alpha + \nu - \mu) \bar{\kappa}_{xy} = 2\alpha \bar{\kappa}_{xy0} \quad (1c)$$

The left side $\bar{\kappa}$ terms are the dimensionless out-of-plane curvatures of the deformed shell where subscripts x and y refer to ordinary curvatures and xy refers to twisting. On the right side are any initial curvatures, denoted by an extra “0” subscript and the *residual* curvatures due to prestressing in orthogonal directions $\bar{\kappa}_{xF}$ and $\bar{\kappa}_{yF}$: again, an overbar denotes a dimensionless quantity.

As carefully described in Ref. [6], prestressing results in permanent bending of the shell and the corresponding residual curvatures describe the shape of the shell if it could deform *freely* without constraint, i.e., without developing elastic bending moments. But the shell cannot do so and deforms elastically to $\bar{\kappa}_x$, $\bar{\kappa}_y$, and $\bar{\kappa}_{xy}$ in order to equilibrate the residual stresses in the absence of any external loads. Thus, the formulation incorporates the residual curvatures as an initial condition, preceding elastic deformation: It also accounts for a twisting prestress but which is not needed here.

The Poisson ratio is ν and the shear modulus relative to the Young’s modulus is α equal to $(1 - \nu)/2$ in the isotropic case but otherwise specifying a *directly isotropic* behavior, which is a special case of orthotropy where the in-plane Young’s moduli are identical. The change in the dimensionless Gaussian curvature $\Delta \bar{g}$ is contained within μ according to

$$\mu = \nu + \phi \Delta \bar{g} = \nu + \phi (\bar{\kappa}_x \bar{\kappa}_y - \bar{\kappa}_{xy}^2 - \bar{\kappa}_{x0} \bar{\kappa}_{y0} + \bar{\kappa}_{xy0}^2) \quad (2)$$

where ϕ is the factor of material stiffness and geometry given by

$$\phi = \frac{b^4}{t^2 R^2} \cdot \frac{(1 - \nu^2)\alpha}{3\alpha + (1 - \nu^2 - 2\nu\alpha)\rho^2 + 3\alpha\rho^4} \quad (3)$$

The ratio of minor-to-major semi-axis lengths b/a is ρ , the thickness of shell is t , and R is the characteristic radius of curvature for making the previous curvatures dimensionless according to $\bar{\kappa} = \kappa R$. Note that when $\phi \gg 1$, the shell is very thin and inextensibility follows.

Equations (1a)–(1c) and Eq. (2) are four coupled nonlinear equations, which are solved for $\bar{\kappa}_x$, $\bar{\kappa}_y$, $\bar{\kappa}_{xy}$ and μ when the initial shape, material parameters, and prestress levels are specified. The stability of all equilibrium solutions found is, then, assured by the matrix of generalized stiffness being positive definite. This matrix has the general and specific forms as

$$\begin{bmatrix} \partial^2 \bar{U} / \partial \bar{\kappa}_x^2 & \partial^2 \bar{U} / \partial \bar{\kappa}_x \partial \bar{\kappa}_y & \partial^2 \bar{U} / \partial \bar{\kappa}_x \partial \bar{\kappa}_{xy} \\ \partial^2 \bar{U} / \partial \bar{\kappa}_y \partial \bar{\kappa}_x & \partial^2 \bar{U} / \partial \bar{\kappa}_y^2 & \partial^2 \bar{U} / \partial \bar{\kappa}_y \partial \bar{\kappa}_{xy} \\ \partial^2 \bar{U} / \partial \bar{\kappa}_{xy} \partial \bar{\kappa}_x & \partial^2 \bar{U} / \partial \bar{\kappa}_{xy} \partial \bar{\kappa}_y & \partial^2 \bar{U} / \partial \bar{\kappa}_{xy}^2 \end{bmatrix} = \begin{bmatrix} 1 + \phi \bar{\kappa}_y^2 & \mu + \phi \bar{\kappa}_y \bar{\kappa}_x & -2\phi \bar{\kappa}_y \bar{\kappa}_{xy} \\ \mu + \phi \bar{\kappa}_x \bar{\kappa}_y & 1 + \phi \bar{\kappa}_x^2 & -2\phi \bar{\kappa}_x \bar{\kappa}_{xy} \\ -2\phi \bar{\kappa}_{xy} \bar{\kappa}_y & -2\phi \bar{\kappa}_{xy} \bar{\kappa}_x & 4\alpha - 2\phi \Delta \bar{g} + 4\phi \bar{\kappa}_{xy}^2 \end{bmatrix} \quad (4)$$

where \bar{U} from Ref. [6] is the total dimensionless strain energy stored in the deformed shell.

3 Opposite-Sense Prestressing

As shown in Fig. 1, the shell is initially flat and is, then, prestressed by plastically curving in opposite senses. The levels of prestress in both directions are taken to be identical for this permits a neat closed form solution, different prestress levels are treated in Sec. 5. Identical prestressing can be availed by setting $\bar{\kappa}_{xF} = -\bar{\kappa}_{yF} = \bar{k}_1$, say, in Eqs. (1a)–(1c) where \bar{k}_1 is referred to as a “prestress” term, henceforth, for simplicity. All other right side terms are equal to zero and

$$\bar{\kappa}_x + \mu \bar{\kappa}_y = \bar{k}_1(1 - \nu) \quad (5a)$$

$$\mu \bar{\kappa}_x + \bar{\kappa}_y = -\bar{k}_1(1 - \nu) \quad (5b)$$

$$(2\alpha + \nu - \mu) \bar{\kappa}_{xy} = 0 \quad (5c)$$

Even though the practical shells are metallic, the relative shear modulus α is, generally, retained. Since there is no twist in practice, it can be assumed that $\bar{\kappa}_{xy} = 0$, which satisfies Eqn. (5c). The symmetry of the first two equations permits another solution in which $\bar{\kappa}_x = -\bar{\kappa}_y = \bar{\kappa}$, say, and either of Eq. (5a) or Eq. (5b) presents

$$\bar{\kappa} + \frac{\phi}{(1 - \nu)} \bar{\kappa}^3 = \bar{k}_1 \quad (6)$$

after replacing μ by $\nu - \phi \bar{\kappa}^2$ using Eq. (2). This is the nonlinear governing equation of opposite-sense bending of the shell where \bar{k}_1 determines $\bar{\kappa}$ monotonically and there is no bistable behavior. Stretching is implied by the cubic term in $\bar{\kappa}$, which accounts for a disproportionate increase in the level of middle-surface strains.

Equations (5a) and (5b) are also satisfied by $\mu = -1$ by inspection. Consequently, they collapse into a single expression $\bar{\kappa}_x - \bar{\kappa}_y = (1 - \nu) \bar{k}_1$ and from the definition of μ , $\bar{\kappa}_x \bar{\kappa}_y = -(1 + \nu) / \phi$. From these two equations, the set of principal curvatures can be solved uniquely as

$$\begin{aligned} \bar{\kappa}_x &= \frac{\bar{k}_1(1 - \nu)}{2} \left[1 \pm \left[1 - \frac{4(1 + \nu)}{\phi \bar{k}_1^2(1 - \nu)^2} \right]^{1/2} \right], \\ \bar{\kappa}_y &= -\frac{\bar{k}_1(1 - \nu)}{2} \left[1 \mp \left[1 - \frac{4(1 + \nu)}{\phi \bar{k}_1^2(1 - \nu)^2} \right]^{1/2} \right] \end{aligned} \quad (7)$$

which are now two equilibrium states depending on the choice of internal signs. The shell can adopt either state but interestingly, the product $\bar{\kappa}_x \bar{\kappa}_y$ for both does not depend on \bar{k}_1 and remains constant. If α assumes its isotropic value of $(1 - \nu) / 2$, then Eq. (5c) is automatically satisfied and $\bar{\kappa}_{xy}$ does not have to be zero but it is taken to be so since there is no observed twist.

The solutions offered by Eqs. (6) and (7) are three valid equilibrium states describing $\bar{\kappa}_x$ and $\bar{\kappa}_y$ (and $\bar{\kappa}_{xy}$), which co-exist at a single value of prestress $\bar{k}_1 = \bar{k}_1^*$, say. For a different prestress, the solutions from either of Eq. (6) or Eq. (7) are stable when the Eigenvalues of the stability matrix in Eq. (4) are positive after substituting back the solution curvatures for each mode. In the case of the nonlinear initial response, the Eigenvalues of the stability matrix can be verified as

$$4\alpha + 2\phi \bar{\kappa}^2, \quad 1 - \nu + 3\phi \bar{\kappa}^2, \quad 1 + \nu - \phi \bar{\kappa}^2 \quad (8)$$

Positive Eigenvalues are obtained when $\bar{\kappa}$ is less than a maximum value of $\bar{\kappa}^*$ equal to $\sqrt{(1 + \nu) / \phi}$, as suggested by the final Eigenvalue above. The value of \bar{k}_1^* is found by substituting $\bar{\kappa}^*$ back into Eq. (6) and re-arranging to reveal

$$\bar{k}_1^* = \sqrt{\frac{4(1 + \nu)}{\phi(1 - \nu)^2}} \quad (9)$$

This critical prestress can be obtained informally from the starting limit on real curvatures in Eq. (7) where real values persist only when $\bar{k}_1 \geq \bar{k}_1^*$. In this case, the formal stability calculation shows that the final matrix entry is itself an Eigenvalue when $\bar{\kappa}_{xy} = 0$ and has a value

$$4\alpha - 2\phi \Delta \bar{g} = 4\alpha + 2(1 + \nu) \quad (10)$$

since $\Delta \bar{g} = -(1 + \nu) / \phi$ via $\mu = -1$. This Eigenvalue is precisely the dimensionless torsional stiffness of the deformed shell $\partial^2 \bar{U} / \partial \bar{\kappa}_{xy}^2$, which is always positive irrespective of the value of material shear modulus provided $\alpha > 0$. Physically, when the metallic shell in Fig. 1 rests in either equilibrium shape, it is torsionally stiff enough to stabilize against any perturbations of a twisting nature. Finally, it is noted that for high levels of prestress or when inextensibility prevails, such that \bar{k}_1 and/or ϕ are large, the asymptotic solutions are $(\bar{\kappa}_x, \bar{\kappa}_y) \rightarrow (\bar{k}_1[1 - \nu], 0)$ or, equally valid, $(\bar{\kappa}_x, \bar{\kappa}_y) \rightarrow (0, -\bar{k}_1[1 - \nu])$, which testify to the orthogonal cylindrical modes reported in Fig. 1.

4 Same-Sense Prestressing

Again, the shell is initially flat but prestressing is in the same sense, to the same degree, and is declared by setting $\bar{\kappa}_{xF} = \bar{\kappa}_{yF}$ equal to \bar{k}_2 in the governing equations, which become

$$\bar{\kappa}_x + \mu \bar{\kappa}_y = \bar{k}_2(1 + \nu) \quad (11a)$$

$$\mu \bar{\kappa}_x + \bar{\kappa}_y = \bar{k}_2(1 + \nu) \quad (11b)$$

$$(2\alpha + \nu - \mu) \bar{\kappa}_{xy} = 0 \quad (11c)$$

When α is not isotropic in value, then $\bar{\kappa}_{xy}$ must be zero to satisfy Eq. (11c); however, this may not be the case when $\alpha = (1 - \nu) / 2$ since the metallic shell in Fig. 2 can be twisted: these cases are treated momentarily.

The symmetry of the first two equations admits a natural solution $\bar{\kappa}_x = \bar{\kappa}_y$, equal to $\bar{\kappa}$ whereupon substituting into μ and, then, into either of Eq. (11a) or Eq. (11b), produces

$$\bar{\kappa} + \frac{\phi}{1+\nu} \bar{\kappa}^3 = \bar{k}_2 \quad (12)$$

Compared to Eq. (6), this expression also describes the nonlinear bending of the shell but with a different cubic coefficient.

Equations (11a) and (11b) are also satisfied by $\mu=1$, which is an automatic solution of Eq. (11c) in the isotropic case: $\bar{\kappa}_{xy} \neq 0$ for $\alpha=(1-\nu)/2$ but $\bar{\kappa}_{xy}=0$ for other values of α . Both of these cases can be treated together by introducing, in the isotropic case, a new axes set X and Y suitably rotated from x and y about z and aligned to the directions of principal curvature $\bar{\kappa}_X$ and $\bar{\kappa}_Y$. A Mohr's circle asserts that $\bar{\kappa}_x + \bar{\kappa}_y = \bar{\kappa}_X + \bar{\kappa}_Y$, $(\bar{\kappa}_x \bar{\kappa}_y - \bar{\kappa}_{xy}^2) = \bar{\kappa}_X \bar{\kappa}_Y$, and $\bar{\kappa}_{XY} = 0$. Equations (11a) and (11b) can now be combined to yield $\bar{\kappa}_X + \bar{\kappa}_Y = \bar{k}(1+\nu)$ and $\bar{\kappa}_X \bar{\kappa}_Y = (1-\nu)/\phi$ from setting $\mu=1$ and when α is not isotropic, the same expressions arise wherein the subscripts X and Y are interchanged with x and y , respectively, which is implied in the following solutions. Solving for both principal curvatures produces

$$\begin{aligned} \bar{\kappa}_X &= \frac{\bar{k}_2(1+\nu)}{2} \left[1 \pm \left[1 - \frac{4(1-\nu)}{\phi \bar{k}_2^2(1+\nu)^2} \right]^{1/2} \right], \\ \bar{\kappa}_Y &= \frac{\bar{k}_2(1+\nu)}{2} \left[1 \mp \left[1 - \frac{4(1-\nu)}{\phi \bar{k}_2^2(1+\nu)^2} \right]^{1/2} \right] \end{aligned} \quad (13)$$

These are valid equilibrium states when \bar{k}_2 assumes a value larger than a critical value \bar{k}_2^* where

$$\bar{k}_2^* = \sqrt{\frac{4(1-\nu)}{\phi(1+\nu)^2}} \quad (14)$$

Note the similarity to Eq. (9) and, as with opposite-sense prestressing, the product, $\bar{\kappa}_X \bar{\kappa}_Y$ is always a constant irrespective of the level of \bar{k}_2 when $\bar{k}_2 \geq \bar{k}_2^*$. The stability performance is formally obtained by reconstructing the elements of the matrix in Eq. (4) in the X - Y system by replacing $\bar{\kappa}_x$, $\bar{\kappa}_y$, and $\bar{\kappa}_{xy}$ with $\bar{\kappa}_X$, $\bar{\kappa}_Y$, and $\bar{\kappa}_{XY}$ and setting $\bar{\kappa}_{XY}=0$.

When $\bar{k}_2 < \bar{k}_2^*$, it is straightforward to show that the mode described by Eq. (12) is stable. When $\bar{k}_2 \geq \bar{k}_2^*$, the least positive Eigenvalue is, again, the final matrix entry in Eq. (4), of value

$$4\alpha - 2\phi\Delta\bar{g} = 4\alpha - 2(1-\nu) \quad (15)$$

since $\Delta\bar{g}=(1-\nu)/\phi$ from $\mu=1$. In the isotropic case, this Eigenvalue is always zero and because it is also the deformed torsional stiffness, this result confirms the twisting neutrally stable shell in Fig. 2. If the relative shear modulus is greater than $(1-\nu)/2$, the shell is bistable where the curvatures, now aligned to original x and y coordinates, adopt either of the values in Eq. (13) according to the order of the internal signs. The asymptotic values show that the curvatures clearly diverge such that when \bar{k}_2 becomes large or $\phi \gg 1$, then $(\bar{\kappa}_x, \bar{\kappa}_y) \rightarrow (\bar{k}_2[1+\nu], 0)$ or $(\bar{\kappa}_x, \bar{\kappa}_y) \rightarrow (0, \bar{k}_2[1+\nu])$ and the shell is cylindrically curved about one of two orthogonal directions in the same sense.

5 Disparate Prestressing

The previous cases assume that the levels of prestress are identical, irrespective of the direction of residual bending they produce about the x and y directions. Now, consider the case when prestressing can be generally specified according to

$$\bar{k}_3 = \bar{\kappa}_{xF} + \nu \bar{\kappa}_{yF}, \quad \bar{k}_4 = \nu \bar{\kappa}_{xF} + \bar{\kappa}_{yF} \quad (16)$$

where the governing equations can be written

$$\bar{\kappa}_x + \mu \bar{\kappa}_y = \bar{k}_3 \quad (17a)$$

$$\mu \bar{\kappa}_x + \bar{\kappa}_y = \bar{k}_4 \quad (17b)$$

$$(2\alpha + \nu - \mu) \bar{\kappa}_{xy} = 0 \quad (17c)$$

When the shell is initially flat, note that α is generally retained in Eq. (17c).

In these expressions, there are no obvious solutions apart from $\bar{\kappa}_{xy}=0$ and, hence, it is necessary to solve explicitly for $\bar{\kappa}_x$ and $\bar{\kappa}_y$ between Eqs. (17a) and (17b) and to substitute the expressions back into Eq. (2) in order to reveal a characteristic polynomial equation in μ . This produces

$$\bar{\kappa}_x = \frac{\bar{k}_3 - \mu \bar{k}_4}{1 - \mu^2} \quad (18a)$$

$$\bar{\kappa}_y = \frac{\bar{k}_4 - \mu \bar{k}_3}{1 - \mu^2} \quad (18b)$$

$$\Rightarrow (\mu - \nu)(1 - \mu^2)^2 - \phi(\bar{k}_3 - \mu \bar{k}_4)(\bar{k}_4 - \mu \bar{k}_3) = 0 \quad (18c)$$

The roots of the polynomial produce values of μ for individual equilibrium cases, which define the deformed curvatures via Eqs. (18a) and (18b) whose stability is assessed via the Eigenvalues of Eq. (4). Roots in closed form are not available for \bar{k}_3 and \bar{k}_4 , generally, but are obtained numerically using the software package MATLAB [8], which is also used to compute the eigenvalues. Figure 3 shows the corresponding results for circular shells for a range of prestress when there are three values of relative shear modulus, which approach the isotropic value: $\alpha=4 \times (1-\nu)/2$, $1.1 \times (1-\nu)/2$, and $1.01 \times (1-\nu)/2$. In each subfigure, the color shading indicates the number of stable shapes found for each combination of prestress.

When (\bar{k}_3, \bar{k}_4) are both positive and negative, same-sense prestressing arises: When they differ in sign, prestressing is in the opposite sense. Therefore, the first and third quadrants in each subfigure in Fig. 3 show the same results, as do the second and fourth quadrants. All quadrants display either monostable or bistable shells and bistability is, generally, accorded when a certain threshold of prestress is surpassed. Specifically, the bistable region emanates from a single point in each quadrant whose coordinates are equal in size and the levels of prestress are the same at these origin points, which are identified as \bar{k}_3^* and \bar{k}_4^* , respectively. For opposite-sense prestressing, Eq. (9) suggests

$$\bar{k}_3^*, \quad \bar{k}_4^* = \bar{k}_1^*(1-\nu) \Rightarrow \bar{k}_3^*, \quad \bar{k}_4^* = \sqrt{4(1+\nu)/\phi} \quad (19)$$

and from Eq. (14) for same-sense prestressing

$$\bar{k}_3^*, \quad \bar{k}_4^* = \bar{k}_2^*(1+\nu) \Rightarrow \bar{k}_3^*, \quad \bar{k}_4^* = \sqrt{4(1-\nu)/\phi} \quad (20)$$

Both sets of points are duly indicated on Fig. 3 for confirmation.

For the largest α , there is little difference between the effects of opposite-sense and same-sense prestressing. As α reduces, the size of the same-sense bistable region diminishes so that when α is very close to its isotropic value, bistability is governed by the limiting condition of $\bar{k}_3 = \bar{k}_4$: For marginal differences in prestress, the shell is monostable. However, when the relative shear stiffness is exactly isotropic, recall from Sec. 4 that neutral stability occurs only when $\bar{k}_3 = \bar{k}_4$, thereby, confirming the precision required for making practical neutrally stable shells. On the other hand, the relatively indifferent behavior under opposite-sense prestress when α changes suggests that bistable shells can be more simply made provided the levels are large enough and not too dissimilar.

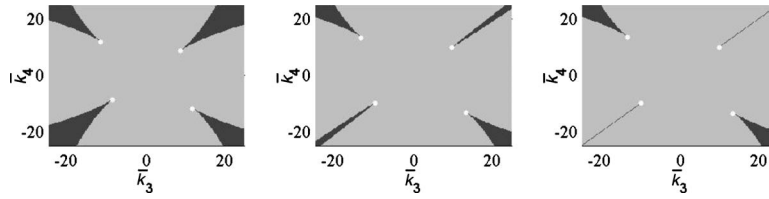


Fig. 3 Stability landscape for originally flat shells with prestress levels \bar{k}_3 and \bar{k}_4 in orthogonal directions according to Eq. (16). Each subplot refers to a specific value of the relative shear modulus, α : left, $4 \times (1 - \nu)/2$; middle, $1.1 \times (1 - \nu)/2$; right, $1.01 \times (1 - \nu)/2$ (the isotropic value being $(1 - \nu)/2$). All of the darkest regions conform to bistable shells and the lightest are monostable. The first and third quadrants in each subfigure are mirror symmetrical in both axes, as are the second and fourth quadrants. The white points denote the closed form solutions asserting the onset of bistable behavior when the levels of prestress are identical, given by Eq. (20) (first and third) and Eq. (19) (second and fourth). The value of ϕ is given by Eq. (3) where a circular shell is taken with $\rho=1$ and $b^4/l^2 R^2$ is set to a nominal value of unity. The Poisson's ratio is set to 0.3.

6 Effect of Initial Curvature

As a final exercise, the performance of initially curved, stress-free shells, which are, then, prestressed in the same sense, is considered in more detail. For simplicity, the shell is a spherical cap and the prestress levels are identical for this enables a range of results to be presented compactly. Moreover, the material is taken to be isotropic in order to compare the influence of initial shape with the initially flat, neutrally stable shells of Sec. 4. In this case, $\bar{\kappa}_{xF}$ and $\bar{\kappa}_{yF}$ are set equal to \bar{k}_5 , $\bar{\kappa}_{x0} = \bar{\kappa}_{y0} = \bar{\kappa}_0$, and $\bar{\kappa}_{xy0} = 0$. The governing equations of deformation for material isotropy are

$$\bar{\kappa}_x + \mu \bar{\kappa}_y = (\bar{\kappa}_0 + \bar{k}_5)(1 + \nu) \quad (21a)$$

$$\mu \bar{\kappa}_x + \bar{\kappa}_y = (\bar{\kappa}_0 + \bar{k}_5)(1 + \nu) \quad (21b)$$

$$(1 - \mu) \bar{\kappa}_{xy} = 0 \quad (21c)$$

As in Sec. 4, $\mu=1$ is a valid solution by inspection with

$$\bar{\kappa}_x = \frac{(\bar{\kappa}_0 + \bar{k}_5)(1 + \nu)}{2} \left[1 \pm \left[1 - \frac{4(1 - \nu) + 4\phi \bar{\kappa}_0^2}{\phi(\bar{\kappa}_0 + \bar{k}_5)^2(1 + \nu)^2} \right]^{1/2} \right],$$

$$\bar{\kappa}_y = (\bar{\kappa}_0 + \bar{k}_5)(1 + \nu) - \bar{\kappa}_x \quad (22)$$

As discussed previously, $\bar{\kappa}_{xy}$ may not be zero when $\mu=1$ but there exists a principal set of X - Y axes for which $\bar{\kappa}_{XY}$ is zero and the other curvatures $\bar{\kappa}_X$ and $\bar{\kappa}_Y$ have the same expressions immediately above. Thus, $\bar{\kappa}_{xy}$ is set to zero for convenience.

For other solutions in which $\mu \neq 1$, the following third order characteristic equation can be found by solving explicitly for the curvatures in Eqs. (21a)–(21c) and substituting into Eq. (2)

$$(\mu - \nu + \phi \bar{\kappa}_0^2)(1 + \mu)^2 - \phi(\bar{\kappa}_0 + \bar{k}_5)^2(1 + \nu)^2 = 0 \quad (23)$$

The roots in μ can be determined numerically and back-substituted to reveal the deformed curvatures whose stability is confirmed in the usual way via the positive definiteness of Eq. (4). Results are indicated by the stability landscape shown in Fig. 4 constructed as per Fig. 3 for a range of $\bar{\kappa}_0$ and \bar{k}_5 for shells with circular planforms. Accordingly, the performance of the originally flat shell in Sec. 4 is embraced.

When the prestress is moderate $\bar{k}_5 < 4$, shallow shells are monostable and bend spherically in the same direction as the prestress. Bistability under prestress is, then, achieved when the magnitude of the initial curvature is large enough: The shell is also bistable when there is no prestress, as noted originally by Wittrick et al. [9] and more lately by Seffen and McMahon [10]. The required threshold of initial curvature has to be greater than $\bar{\kappa}_0^*$

$= \sqrt{4(1 + \nu)/\phi}$, which can be found by solving either of Eq. (21a) or Eq. (21b) with $\bar{\kappa}_x = \bar{\kappa}_y$ and $\bar{k}_5 = 0$ for real and stable solutions. Otherwise, the boundary between monostable regions and bistable regions increases gently and monotonically for positively curved shells but for negatively curved shells, it behaves differently with a notable cusp in a region close to $\bar{k}_5 = 4$.

When $\bar{k}_5 > 4$, there are five possible responses depending on the size and sign of the initial curvature. Shells with the deformed curvatures of Eq. (22) are neutrally stable provided

$$\bar{k}_5 \geq -\bar{\kappa}_0 + \frac{2}{1 + \nu} [(1 - \nu)/\phi + \bar{\kappa}_0^2]^{1/2} \quad (24)$$

which is calculated from the same expressions being valid and real but which is also confirmed numerically during solution of the characteristic polynomial. Highly curved shells are bistable but if the prestress level is large enough under positive $\bar{\kappa}_0$, then, it overlaps with the neutrally stable region, as indicated. From examining the general form of the solution curvatures, the shell is neutrally stable as before in a torsional mode or it can occupy a stable inverted shape: Essentially, one of the stable shapes within the bistable mode becomes neutrally stable. Negatively curved

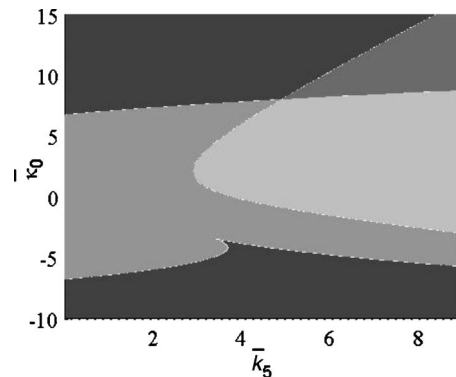


Fig. 4 Regions of stable equilibria for shells with combinations of same-sense prestressing \bar{k}_5 and initial spherical curvature $\bar{\kappa}_0$. The darkest regions conform to bistable configurations. The lightest region exhibits neutral stability whilst the second darkest regions in the top-right corner of the subfigure are configurations that possess a neutrally stable mode and a singly stable inverted shape. The second lightest regions are monostable configurations only. All shells are circular, $\rho=1$, $b^4/l^2 R^2=1$, and $\nu=0.3$.

shells are neutrally stable only when the prestress is large enough but, generally, they are first monostable and, then, bistable as the size of initial curvature increases.

7 Conclusion

This study has considered the influence of prestress on the bistable capability of thin shells. By tailoring a general set of governing equations of deformation derived in another study, closed form solutions for oppositesense and same-sense prestressing have been obtained. In the case of isotropic material, it has been shown that opposite-sense prestressing invokes bistability when the prestress is large enough whereas for same-sense prestressing, the shell occupies a neutrally stable mode with no torsional stiffness. The latter performance has been observed in heated shells [3,4] but has not been formally quantified as a neutrally stable mode. In the case of the former, it is analogous to a problem arising in the thermal curing of certain fibre-composite shells, first reported by Hyer [11] where residual bending occurs due to the material anisotropy and to in-plane differential contraction. Hyer noted that an initially flat shell distorts into a saddle profile but as the curing temperature increases, this shape becomes unstable and the shell suddenly buckles into a mode dominated by a single curvature, either upward or downward. His determination of the buckling condition was performed numerically; Eqs. (6), (7), and (9) provide elegant closed form solutions for a simpler material specification but, nonetheless, contribute to clarifying Hyer's findings, which many authors cite as seminal research on morphing structures. When the prestress levels are generally different, bistability under opposite-sense prestressing is not affected by the shear modulus of material. On the other hand, same-sense prestressing does depend on the shear modulus; if it is larger than the isotropic value, shells are bistable but within a narrow band of

prestress levels, which grows with increasing shear modulus: When isotropy prevails, the levels of prestress have to be identical for a shell to be neutrally stable, otherwise, it is monostable. Finally, initial curvature alongside prestress has produced an interesting performance range, including a hybrid performance, combining bistability with neutral stability, which is now being validated in practice.

Acknowledgment

We are grateful to Emeritus Professor C. R. Calladine for comments on a first draft of paper, which has helped to reorganize the content here.

References

- [1] Guest, S. D., Kebabdz, E., and Pellegrino, S., 2010, "A Zero-Stiffness Elastic Shell Structure," *Journal of the Mechanics of Materials and Structures*, in press.
- [2] Kebabdz, E., Guest, S. D., and Pellegrino, S., 2004, "Bistable Prestressed Shell Structures," *Int. J. Solids Struct.*, **41**(11–12), pp. 2801–2820.
- [3] Mansfield, E. H., 1962, "Bending, Buckling and Curling of a Heated Thin Plate," *Proc. R. Soc. London, Ser. A*, **268**(1334), pp. 316–327.
- [4] Mansfield, E. H., 1965, "Bending, Buckling and Curling of a Heated Elliptical Plate," *Proc. R. Soc. London, Ser. A*, **288**, pp. 396–417.
- [5] Seffen, K. A., 2007, "Morphing Bistable Orthotropic Elliptical Shallow Shells," *Proc. R. Soc. London, Ser. A*, **463**(2077), pp. 67–83.
- [6] Seffen, K. A., 2008, "Multistable Anisotropic Shells: Governing Equations of Deformation," Engineering Department, Cambridge University, Technical Report No. CUED/D-STRUCT/TR 225.
- [7] Guest, S. D., and Pellegrino, S., 2006, "Analytical Models for Bistable Cylindrical Shells," *Proc. R. Soc. London, Ser. A*, **462**, pp. 839–854.
- [8] MathWorks, 2000, *MATLAB R12*, Natick, MA 01760-2098.
- [9] Wittrick, W. H., Myers, D. M., and Blunden, W. R., 1953, "Stability of a Bimetallic Disk," *Q. J. Mech. Appl. Math.*, **6**(1), pp. 15–31.
- [10] Seffen, K. A., and McMahon, R. A., 2007, "Thermal Buckling of a Uniform Disk," *Int. J. Mech. Sci.*, **49**(2), pp. 230–238.
- [11] Hyer, M. W., 1981, "Calculations of the Room-Temperature Shapes of Unsymmetric Laminates," *J. Compos. Mater.*, **15**, pp. 175–194.